

Research Paper

Cysteine-type cathepsins promote the effector phase of acute cutaneous delayed-type hypersensitivity reactions

Johannes Schwenck^{1,2}, Andreas Maurer^{1,3}, Birgit Fehrenbacher⁴, Roman Mehling¹, Philipp Knopf¹, Natalie Mucha¹, Dennis Haupt¹, Kerstin Fuchs¹, Christoph M. Griessinger¹, Daniel Bukala¹, Julia Holstein⁴, Martin Schaller⁴, Irene Gonzalez Menendez⁵, Kamran Ghoreschi^{4,5}, Leticia Quintanilla-Martinez⁶, Michael Gütschow⁷, Stefan Laufer⁸, Thomas Reinheckel^{9,10}, Martin Röcken⁴, Hubert Kalbacher³, Bernd J Pichler^{1,11}, Manfred Kneilling^{1,4}✉

1. Werner Siemens Imaging Center, Department of Preclinical Imaging and Radiopharmacy Eberhard Karls University, 72076 Tübingen, Germany
2. Department of Nuclear Medicine and Clinical Molecular Imaging, Eberhard Karls University, 72076 Tübingen, Germany
3. Interfaculty Institute of Biochemistry, Eberhard Karls University, 72076 Tübingen, Germany
4. Department of Dermatology, Eberhard Karls University, 72076 Tübingen, Germany
5. Department of Dermatology, Venereology and Allergology, Charité - Universitätsmedizin Berlin, 10117 Berlin, Germany
6. Department of Pathology, Eberhard Karls University, 72076 Tübingen, Germany
7. Pharmaceutical Institute, Pharmaceutical Chemistry I, University of Bonn, 53121 Bonn, Germany
8. Department of Pharmaceutical and Medicinal Chemistry, Institute of Pharmacy, Eberhard Karls University, 72076 Tübingen, Germany
9. Institute of Molecular Medicine and Cell Research, Medical Faculty, Albert-Ludwigs University, 79085 Freiburg, Germany
10. German Cancer Consortium (DKTK), partner site Freiburg and German Cancer Research Center (DKFZ), Heidelberg, Germany
11. German Cancer Consortium (DKTK), partner site Tübingen and German Cancer Research Center (DKFZ), Heidelberg, Germany

✉ Corresponding author: email: manfred.kneilling@med.uni-tuebingen.de; telephone: +49-7071-29-83427; fax: +49-7071-29-4451

© Ivyspring International Publisher. This is an open access article distributed under the terms of the Creative Commons Attribution (CC BY-NC) license (<https://creativecommons.org/licenses/by-nc/4.0/>). See <http://ivyspring.com/terms> for full terms and conditions.

Received: 2018.10.28; Accepted: 2019.03.28; Published: 2019.05.31

Abstract

Cysteine-type cathepsins such as cathepsin B are involved in various steps of inflammatory processes such as antigen processing and angiogenesis. Here, we uncovered the role of cysteine-type cathepsins in the effector phase of T cell-driven cutaneous delayed-type hypersensitivity reactions (DTHR) and the implication of this role on therapeutic cathepsin B-specific inhibition.

Methods: Wild-type, cathepsin B-deficient (*Ctsb*^{-/-}) and cathepsin Z-deficient (*Ctsz*^{-/-}) mice were sensitized with 2,4,6-trinitrochlorobenzene (TNCB) on the abdomen and challenged with TNCB on the right ear to induce acute and chronic cutaneous DTHR. The severity of cutaneous DTHR was assessed by evaluating ear swelling responses and histopathology. We performed fluorescence microscopy on tissue from inflamed ears and lymph nodes of wild-type mice, as well as on biopsies from psoriasis patients, focusing on cathepsin B expression by T cells, B cells, macrophages, dendritic cells and NK cells. Cathepsin activity was determined noninvasively by optical imaging employing protease-activated substrate-like probes. Cathepsin expression and activity were validated *ex vivo* by covalent active site labeling of proteases and Western blotting.

Results: Noninvasive *in vivo* optical imaging revealed strong cysteine-type cathepsin activity in inflamed ears and draining lymph nodes in acute and chronic cutaneous DTHR. In inflamed ears and draining lymph nodes, cathepsin B was expressed by neutrophils, dendritic cells, macrophages, B, T and natural killer (NK) cells. Similar expression patterns were found in psoriatic plaques of patients. The biochemical methods confirmed active cathepsin B in tissues of mice with cutaneous DTHR. Topically applied cathepsin B inhibitors significantly reduced ear swelling in acute but not chronic DTHR. Compared with wild-type mice, *Ctsb*^{-/-} mice exhibited an enhanced ear swelling response during acute DTHR despite a lack of cathepsin B expression. Cathepsin Z, a protease closely related to cathepsin B, revealed compensatory expression in inflamed ears of *Ctsb*^{-/-} mice, while cathepsin B expression was reciprocally elevated in *Ctsz*^{-/-} mice.

Conclusion: Cathepsin B is actively involved in the effector phase of acute cutaneous DTHR. Thus, topically applied cathepsin B inhibitors might effectively limit DTHR such as contact dermatitis or

psoriasis. However, the cathepsin B and Z knockout mouse experiments suggested a complementary role for these two cysteine-type proteases.

Key words: inflammation, proteases, cathepsin B, optical imaging, delayed-type hypersensitivity

Introduction

Proteases are known for their diverse extra- and intracellular functions under both physiological and pathological conditions. Cysteine-type cathepsins, a large family of proteases, were first found in lysosomes and have been considered strict intracellular enzymes that degrade ingested proteins [1]. However, in recent years, complex intra- and extracellular interactions of cathepsins have been discovered [2].

In this study, we focused on cathepsin B, a ubiquitously expressed cysteine exopeptidase [3]. Cathepsin B is expressed as a proenzyme, which is activated in early endosomes by autocatalytic cleavage [3, 4]. In the acidic pH of the endolysosomal cell compartment, cathepsin B is involved in the antigen processing crucial for adaptive immunity. Indeed, the contribution of cathepsin B to Toll-like receptor (TLR) signaling [5], apoptosis [6] and tumor necrosis factor (TNF) secretion [7] is critical for the innate immune response. Although cathepsin B is unstable at neutral pH, several experiments have shown that cathepsin B is involved in extracellular processes such as angiogenesis [8], extracellular matrix remodeling and cell migration [9]. Thus, a wide variety of diseases, such as rheumatoid arthritis [10], multiple sclerosis [11], pancreatitis [12], cancer [13] and Alzheimer's disease [14], are associated with enhanced cathepsin B expression.

Noninvasive optical imaging using protease-activatable probes is a well-established tool to determine the activity of cathepsins *in vivo* [15, 16]. The protease-activatable probe features a peptide sequence preferentially cleaved by the corresponding protease. Cleavage at this site by proteases such as cathepsin B, Z, L or S abolishes the fluorescence resonance energy transfer (FRET)-mediated quenching of the fluorescence signal, enabling the measurement of cathepsin activity by *in vivo* optical imaging [15, 16].

Contact hypersensitivity reactions are cutaneous delayed-type hypersensitivity reactions (DTHR) mediated by interferon (IFN)- γ -producing CD8⁺ (cytotoxic T (Tc)1) and CD4⁺ (T helper (Th)1) cells. Our group extensively studied the role of mast cell TNF secretion [17], matrix metalloproteinase (MMP) activity [18], $\alpha_v\beta_3$ integrin expression and angiogenesis [19] in acute and chronic experimental 2,4,6-trinitrochlorobenzene (TNCB)-induced cutaneous DTHR. Because TNF secretion [7] and

angiogenesis [8] are considered cathepsin B-dependent, this protease seems to be a further candidate target molecule for therapeutic approaches for cutaneous DTHR. To date, no *in vivo* data exist regarding the efficacy of specific topically applied cathepsin B inhibitors in inflammatory processes such as T cell-driven, TNCB-induced cutaneous DTHR. The irreversible cathepsin B inhibitor CA-074 was developed from the broad-spectrum cathepsin inhibitor E-64 [20] and highly selectively inhibits intracellular cathepsin B *in vitro* [21]. To attain enhanced selectivity, CA-074 interacts with amino acids in the characteristic structural feature of cathepsin B, the occluding loop, as does the recently designed inhibitor 17 [22].

In this study, we focused on the *in vivo* sites of cathepsin activity and the identification of cathepsin B-expressing inflammatory cells at the inflammation sites and draining lymph nodes. To our knowledge, the topical application of cathepsin B inhibitors has not yet been tested. Here, we investigated the efficacy of the topical, highly specific cathepsin B inhibitors CA-074 and inhibitor 17 to suppress ear swelling responses in TNCB-induced experimental cutaneous DTHR.

Materials and Methods

Animals

In this study, we used 8- to 12-week-old female C57BL/6 mice (Charles River Laboratories, Sulzfeld, Germany). Cathepsin B-deficient (Ctsb^{-/-}) and cathepsin Z-deficient (Ctsz^{-/-}) mice were backcrossed to the C57BL/6 genetic background for 10 generations [23, 24]. All animal experiments and methods were approved by the Regierungspräsidium Tübingen and were performed in accordance with relevant guidelines and regulations.

In vivo experiments

We sensitized mice on the shaved abdomen (size, approximately 2 cm × 2 cm) by applying 80 μ L of 5% TNCB dissolved in a 4:1 mixture of acetone/Miglyol 812 (SASOL, Witten, Germany). To elicit acute cutaneous DTHR, the animals were challenged with 20 μ L of 1% TNCB (dissolved in a 1:9 mixture of acetone/Miglyol 812) on both sides of the right ear seven days later. The TNCB ear challenge was repeated every 2-3 days on the right ear, up to five times, to induce chronic cutaneous DTHR. As a

control, naïve (nonsensitized) mice were challenged with 1% TNCB on the right ear (irritant-toxic reaction). We measured the ear thickness with a micrometer (Kroeplin, Schlüchtern, Germany) and quantified ear swelling by subtracting the ear thickness before ear challenge from the ear thickness 12 h to 24 h after ear challenge.

Treatment approach

The cathepsin B inhibitor CA-074 (PeptaNova, Sandhausen, Germany) and a newly developed cathepsin B inhibitor, called inhibitor 17 [25], were dissolved in a 1:9 mixture of acetone/Miglyol 812 (SASOL), and 20 μ L of the 0.1 mM CA-074 or 0.1 mM inhibitor 17 solution was applied topically to the right ear every 24 h starting three days prior to the first TNCB ear challenge. As the sham-treatment, we used a 9:1 mixture of acetone/Miglyol 812 (SASOL).

Histology

We sacrificed mice 24 h after TNCB ear challenge and fixed the ear tissue in 4% buffered formalin. We embedded the tissue in paraffin, cut 5- μ m sections using a microtome (Leica, Wetzlar, Germany) and performed hematoxylin and eosin (H&E)-staining according to standard procedures [26].

Optical imaging

In vivo cathepsin activity was measured by optical imaging using a ProSense activatable fluorescent probe, the corresponding noncleavable control probe and CatB680 (PerkinElmer, Waltham, USA). We injected the probes intravenously 12 h after TNCB ear challenge and performed *in vivo* optical imaging measurements 24 h later according to the recommendation of the manufacturer. For optical imaging, a Hamamatsu Aequoria Dark Box and a C4880 Hamamatsu dual mode cooled CCD camera (Hamamatsu Photonics Deutschland GmbH, Herrsching, Germany) were used. During the measurement, mice were anesthetized by the inhalation of isoflurane-O₂ (1.5%; Forane, Abbott GmbH, Wiesbaden, Germany) and heated to maintain the body temperature between 36 °C and 37 °C.

For the appropriate determination of signal intensity (SI) by optical imaging, we carefully fixed the ears planar on a flat black plate using a nylon thread [18]. Regions of interest (ROI) were drawn on the images of the TNCB-challenged right ear and the untreated left ear (internal control) and analyzed semiquantitatively using Wasabi imaging software (Hamamatsu).

Fluorescence microscopy

Mouse ears and (cervical) draining lymph nodes were collected 24 h after the first TNCB ear challenge,

placed in RPMI (Biochrom, Berlin, Germany) and immediately frozen in liquid nitrogen. Skin biopsies were taken from patients with plaque psoriasis. The biomaterial collection study was approved by the ethics committee of Eberhard Karls University (protocol 545/2014BO2), and patients provided written informed consent. Frozen sections were fixed with periodate-lysine-paraformaldehyde (0.1 M L-lysine-HCl; 2% paraformaldehyde; and 0.01 M sodium metaperiodate, pH 7.4). Sections were blocked using donkey serum and were then incubated with the following primary antibodies (Ab): rabbit anti-cathepsin B (1:20, antibodies-online GmbH, Aachen, Germany), goat anti-CD20 (1:50, Santa Cruz Biotechnology, Dallas, USA), mouse anti-CD20 (1:100, Agilent, Santa Clara, USA), goat anti-CD3- ϵ (1:50, Santa Cruz Biotechnology), hamster anti-49b-Alexa Fluor 647 (Biolegend, San Diego, USA), rabbit anti-CD56 (1:100, Cell Marque, Rocklin, USA), rat anti-F4/80 (1:100, Abcam, Cambridge, UK), mouse anti-CD163 (1:100, DCS, Hamburg, Germany), Armenian hamster anti-CD11c-Alexa Fluor 647 (BioLegend) and rabbit anti-Factor XIIIa (1:100, DCS, Hamburg, Germany). Bound antibodies were visualized using Dylight 549- and Dylight 649-conjugated donkey anti-rabbit IgG (Dianova, Hamburg, Germany), Cy3-conjugated donkey anti-rabbit IgG (Dianova), Cy5-conjugated donkey anti-goat IgG (Dianova), Cy5-conjugated donkey anti-mouse IgG (Dianova), Dylight 549-conjugated donkey anti-rat IgG (Dianova), Cy3-conjugated donkey anti-goat IgG (Dianova) and Alexa 647-conjugated donkey anti-rabbit IgG (Dianova) antibodies. For nuclear staining, we used Yopro (1:2000, Invitrogen, Carlsbad, USA) and mounted the slides using Mowiol (Hoechst, Frankfurt, Germany). Sections were analyzed using an LSM 800 (Zeiss, Oberkochen, Germany) or a Leica TCS-SP/Leica DM RB confocal laser scanning microscope (Leica Microsystems, Wetzlar, Germany) and an HCX PL APO 63 \times /1.132-0.6 oil CS objective lens. Images were processed with Leica Confocal Software (LCS, version 2.61). The original magnification was \times 63. Cells double positive for cathepsin B and the specific cell surface antigen were counted in representative areas, and the means are displayed as a percentage of the mean of all cells expressing the specific cell surface antigen.

Active site labeling

Mouse ears and draining lymph nodes were collected 24 h after the first TNCB ear challenge and homogenized in lysis buffer (100 mM citrate/phosphate; 2 mM EDTA; 1% NP40, pH 5) using an Ultra-Turrax disperser (IKA-Werke, Staufen,

Germany). Lysates were cleared by centrifugation (20800 g, 10 min) and stored at -80 °C. Active site labeling of cysteine proteases was performed as previously described [27]. Briefly, 10 µg of cellular protein was preincubated for 15 minutes with 12.5 µM E-64d or solvent control (dimethylsulfoxide; DMSO) in the presence of 50 mM dithiothreitol, followed by the addition of 12.5 µM DCG-04 and incubation at room temperature for 30 minutes. Samples were then subjected to reducing SDS-PAGE on minigels containing 15% polyacrylamide, followed by Western blotting. The biotinylated probe was detected on PVDF membranes using either streptavidin-conjugated peroxidase, Amersham ECL Prime substrate and Amersham Hyperfilm ECL photosensitive film (Amersham, GE Healthcare) or IRDye 680LT streptavidin and an Odyssey Sa imaging system (LI-COR Biotechnology, Bad Homburg, Germany; samples from *Ctsb*^{-/-}/*Ctsz*^{-/-}/wild-type mice are shown in Figure 4B). To validate the specificity of the cathepsin B bands, which were identified at 27-30 kDa by active site labeling, we used an anti-cathepsin B antibody (goat anti-cathepsin B, 1:2222; R&D Systems, Minneapolis, USA) and an anti-cathepsin Z antibody (goat anti-cathepsin Z, 1:2222; R&D Systems, Minneapolis, USA) visualized by a donkey anti-goat IgG antibody (LI-COR, Lincoln, USA), as shown in Figure S5. The original blots are shown in Figures S7-S13.

Flow cytometry

Spleens and lymph nodes were passed through a 70 µm cell strainer to achieve a single-cell suspension, which was then washed in phosphate-buffered saline (PBS) supplemented with 1% fetal bovine serum. Spleens were subjected to an additional erythrocyte lysis step with ACK lysing buffer (BioWhittaker, Basel, Switzerland). Cells were counted with a C-Chip disposable counting chamber (NanoEnTek, Seoul, Korea), and 4.5x10⁶ cells per sample were used for staining. For the T cell panel, flow cytometry staining was performed using monoclonal antibodies (mAbs) against the following proteins and conjugated to the indicated fluorophores: V450-CD3, V500-CD45.2, FITC-CD8, PE-CD4, APC-Cy7-CD62L, Fc-Block (all from BD Biosciences, Franklin Lakes, USA), PE-Cy7-CD69 (eBioscience, Santa Clara, USA), and APC-NK1.1 (Miltenyi Biotec, Bergisch Gladbach, Germany). For the myeloid cell panel, PE-F4/80 (BioLegend, San Diego, USA), V500-CD45.2, APC-CD11c, PE-Cy7-CD11b, Fc-Block (all from BD Biosciences), V450-Gr1, FITC-MHC-II, and APC-Cy7-CD19 (all from eBioscience) were used. Single-cell suspensions were input to a BD LSR Fortessa (BD Biosciences), and analysis was

performed using FlowJo software (Ashland, USA).

For intracellular flow cytometry (Figure S1) ears and draining cervical lymph nodes were collected 24 h after the first TNCB ear challenge. The ears were cut into very small pieces and incubated in a digestion mix containing collagenase IV (Worthington, Lakewood, USA) and DNase I (Sigma, St. Louis, USA) in RPMI (Biochrom, Berlin, Germany). After tissue digestion, the ears and lymph nodes were passed through a 70 µm cell strainer to achieve a single-cell suspension, which was then washed with FACS buffer (phosphate-buffered saline supplemented with 2 % fetal bovine serum and 5 mM EDTA). Non-specific bindings were blocked using Fc-Block (BioLegend, San Diego, USA) and donkey serum (Millipore, Burlington, USA). Surface and viability staining was performed using following antibodies and dyes: Pacific Blue™-CD3, PE-CD19, PE-Cy7-NK1.1 (all from BioLegend, San Diego, USA), Fixable Viability Dye eFluor™ 520 (eBioscience, Santa Clara, USA). For intracellular staining, cells were fixed with 2 % Formaldehyde and cell membrane was permeabilized by incubation with 90 % Methanol followed by washing with FACS buffer containing 0.5 % Saponin. Cells were then incubated with goat-anti-cathepsin B antibody 1:1000 (R&D Systems, Minneapolis, USA) and donkey anti-goat-Alexa Fluor 647 1:800 (Dianova, Hamburg, Germany) was used as secondary antibody. For negative control, cells were incubated only with the secondary antibody. The expression of cell surface antigens and cathepsin B was analyzed by LSRII flow cytometer (BD Biosciences, Heidelberg, Germany) and FlowJo software (Ashland, USA).

Statistical analysis

An unpaired, two-tailed Student's t-test was used to compare the optical imaging signal intensities (Figure 1B right/left ear; Figure S2B/D, CA-074/sham-treatment; Figure S5A, *Ctsb*^{-/-}/wild-type mice).

To analyze the differences in the optical imaging signal intensities between the inflamed right ears of mice with irritative-toxic reactions and cutaneous DTHR after 1, 3 and 5 challenges, we used one-way analysis of variance (ANOVA; Figure 1D). Differences in the ear swelling responses were compared by an unpaired, two-tailed Student's t-test (Figure 4A). According to Bonferroni correction for multiple comparisons, the significance level was adjusted to $p < 0.0125$.

Differences in the ear swelling responses between the sham- and CA-074-treated groups with chronic cutaneous DTHR were compared by Dunnett's test (Figure S2A). We analyzed the ear swelling responses between *Ctsb*^{-/-} and wild-type

mice with acute cutaneous DTHR using an unpaired, two-tailed Student's t-test with Bonferroni correction of the significance level ($p < 0.025$) due to multiple comparisons (Figure 5A; Figure S3A). *Ctsz*^{-/-} mice were compared only qualitatively due to the small sample size (Figure 5A).

Quantitative data are reported as the means \pm standard errors of the mean (SEMs).

Results

In vivo protease activity in acute and chronic TNCB-induced cutaneous DTHR

To measure protease activity in chronic cutaneous DTHR induced in mice by five TNCB challenges, we employed noninvasive imaging of ears using a substrate-like protease-activated probe (ProSense). This probe can be cleaved by several proteases and subsequently detected by fluorescence-based optical imaging [28]. ProSense or

the noncleavable control probe was injected 12 h after the fifth challenge, and optical imaging was performed 24 h later. We found a 4-fold increase in protease activity in the inflamed right ear compared with that in the untreated left ear. In contrast, the noncleavable control probe produced only a very faint background signal, indicating that only the cleavable probe emits a signal of reasonable intensity (Figure 1A/B).

Considering that proteases are significantly activated during chronic cutaneous DTHR, we focused on the specific participation of cathepsins using an optical imaging probe preferentially cleaved by cathepsin B (CatB680) but cleavable to a lesser extent, by other cathepsins, such as cathepsin S [29]. The ear tissue of an untreated naïve control mouse yielded a faint fluorescence signal corresponding to low cathepsin activity in healthy tissue (Figure 1C/D). In the ear with acute cutaneous DTHR elicited by one TNCB challenge one week after sensitization, the

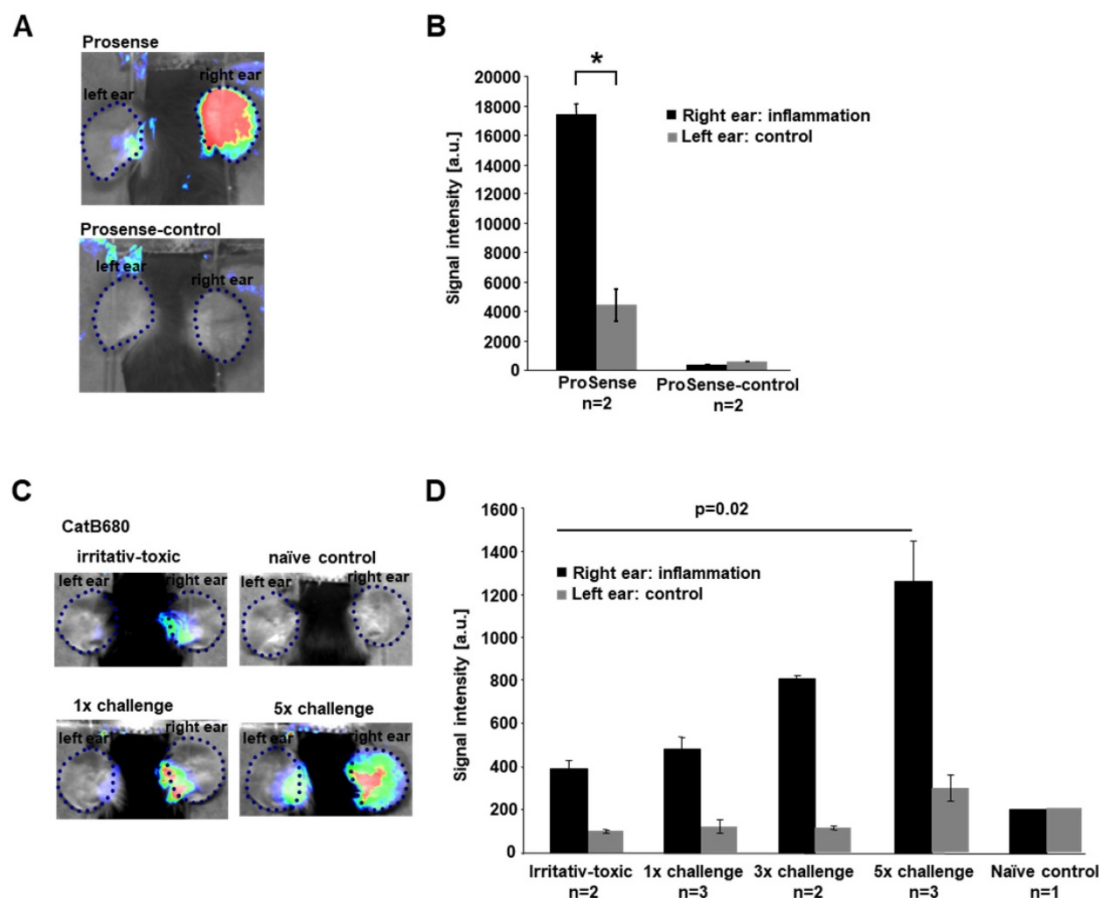


Figure 1: *In vivo* imaging of proteases in cutaneous DTHR. Mice were sensitized with 5% TNCB on the abdomen and, after one week, were challenged with 1% TNCB on the right ear to induce acute cutaneous DTHR. As a control, nonsensitized mice were challenged with 1% TNCB on the right ear (irritative-toxic reaction). To induce chronic cutaneous DTHR, mice were repetitively challenged every two days, up to five times. **A:** ProSense, a probe activatable by several proteases, and ProSense-control, a nonactivatable probe, were injected 12 h after the fifth challenge, and *in vivo* optical imaging was performed 24 h later. **B:** The ProSense signal intensity was 4-fold higher in the inflamed right ears than in the control left ears. The nonactivatable control probe displayed almost no signal (n=2; unpaired, two-tailed Student's t-test; mean \pm SEM). **C/D:** The signal intensity of CatB680, a probe preferentially activated by cathepsin B, was measured after the first, third and fifth TNCB challenges. After the first challenge, the signal intensity was 4-fold higher than that in untreated control ears. After the third and fifth challenges, the signal intensity increased to 400% and 620% of the control signal intensity (one-way ANOVA; mean \pm SEM). Unsensitized mice, which developed an irritative-toxic reaction after a single challenge, showed a slightly lower signal than sensitized mice. Untreated naïve mice showed signal intensities similar to those in the untreated left ears.

CatB680 signal was 4-fold higher than that in the healthy ear. However, this signal was only slightly higher than that in the ears of nonsensitized naïve mice after a single TNCB challenge (nonspecific irritative-toxic control; Figure 1C/D). Ongoing accelerated chronic cutaneous DTHR was associated with an almost linear increase in the CatB680 signal intensity. After five TNCB ear challenges, the signal intensity in chronically inflamed right ears was 2.6-fold higher than that in ears with acute cutaneous DTHR. Importantly, in this context, the signal intensity in the control ears of mice challenged with TNCB five times on the contralateral ears was slightly increased as a consequence of some degree of TNCB spread caused by the cleaning behavior of the experimental mice (Figure 1C/D).

Cellular sources of cathepsin B in acute cutaneous DTHR

To determine the cellular sources of cathepsin B in acute cutaneous DTHR, we conducted immunofluorescence microscopy analyses of ears and draining lymph nodes obtained 24 h after a single TNCB ear challenge. Based on cell surface marker expression, we focused on cathepsin B expression in dendritic cells (DCs; CD11c), B cells (CD20), T cells (CD3), macrophages (F4/80), and NK cells (CD49b). For quantification, we assessed the percentage of cathepsin B-positive CD11c-, CD20-, CD3-, F4/80- and CD49b-expressing cells (Figure 2A). In the healthy ears of naïve mice, which exhibited neither histopathological signs of inflammation nor a leukocytic infiltrate, we could identify almost no cathepsin B-expressing resident cells. However, in ears with acute TNCB-induced cutaneous DTHR, we found strong edema, as well as extensive infiltration of inflammatory cells, as reported by Schwenck et al. [18]. In the present study, cathepsin B expression was detected in 36% of CD11c-positive cells (mainly dendritic cells), 27% of CD20-positive B cells, 26% of CD3-positive T cells, 25% of F4/80-positive macrophages and 15% of CD49b-positive NK cells in ear tissue with acute TNCB-induced cutaneous DTHR (Figure 2A/B). Interestingly, acute cutaneous DTHR was associated with an impressively higher percentage of cathepsin B-positive inflammatory cells in draining lymph nodes than in inflamed ear tissue (Figure 2C). Specifically, in lymph nodes, we detected cathepsin B expression in 73% of dendritic cells, 64% of B cells, 63% of T cells, 80% of macrophages and 64% of NK cells (Figure 2C). Even in lymph nodes of naïve healthy mice, 11% of dendritic cells, 27% of B cells, 38% of T cells, 6% of macrophages and 53% of NK cells stained positive for cathepsin B (Figure 2D). Importantly, in this context, cathepsin B was found

within the cell cytoplasm as well as in the extracellular space. Intracellular cathepsin B flow cytometry analysis revealed a strong cathepsin B expression in the leucocytes with high granularity (most probably neutrophils) isolated from the inflamed ears with acute cutaneous DTHR (Figure S1).

To determine whether our results are applicable to human disease, we analyzed skin tissue from a patient suffering from psoriasis. Like experimental cutaneous DTHR in mice, psoriatic lesions were dominated by neutrophils (Figure 3A). Immunofluorescence microscopy revealed notable cathepsin B expression in B cells, dendritic cells, T cells and NK cells, in accordance with our murine data (Figure 3B).

Specific cathepsin inhibition suppresses acute but not chronic cutaneous DTHR

To address the role of cathepsin B expression and the therapeutic potential of cathepsin B inhibition in acute and chronic cutaneous DTHR, we topically treated TNCB-sensitized mice with the cathepsin B inhibitor CA-074 twice daily. This compound irreversibly inactivates its target, cathepsin B, selectively at nanomolar concentrations but tends to inhibit multiple cysteine-type cathepsins at higher concentrations. We started topical CA-074 treatment four days after sensitization and three days prior to the first TNCB ear challenge to ensure no impairment of the sensitization phase and to achieve a sufficient degree of cathepsin B inhibition. Topically administered CA-074 significantly reduced the ear swelling responses 12 h and 24 h after the first TNCB challenge (Figure 4A) but displayed no significant therapeutic effect on chronic cutaneous DTHR (Figure S2A). In contrast, histological H&E staining of CA-074-treated ears with acute cutaneous DTHR revealed strong reductions in ear thickness, edema, hyperkeratosis, acanthosis and inflammatory cell infiltration of compared with these features in sham-treated ears (Figure 4B). Interestingly, noninvasive *in vivo* optical imaging of CA-074-treated mice using the CatB680 probe showed that the signal intensity in the inflamed ears was not significantly reduced compared to that in the ears of wild-type mice (Figure S2B), suggesting that other proteases may be involved in the activation of the CatB680 optical imaging probe (see discussion). *Ex vivo* optical imaging of draining lymph nodes revealed a tendency towards decreased CatB680 signal intensity, while the contralateral cervical, axillary, inguinal and mesenteric lymph nodes and the thymus, including the perithymic lymph nodes, remained unaffected (Figure S2C/D).

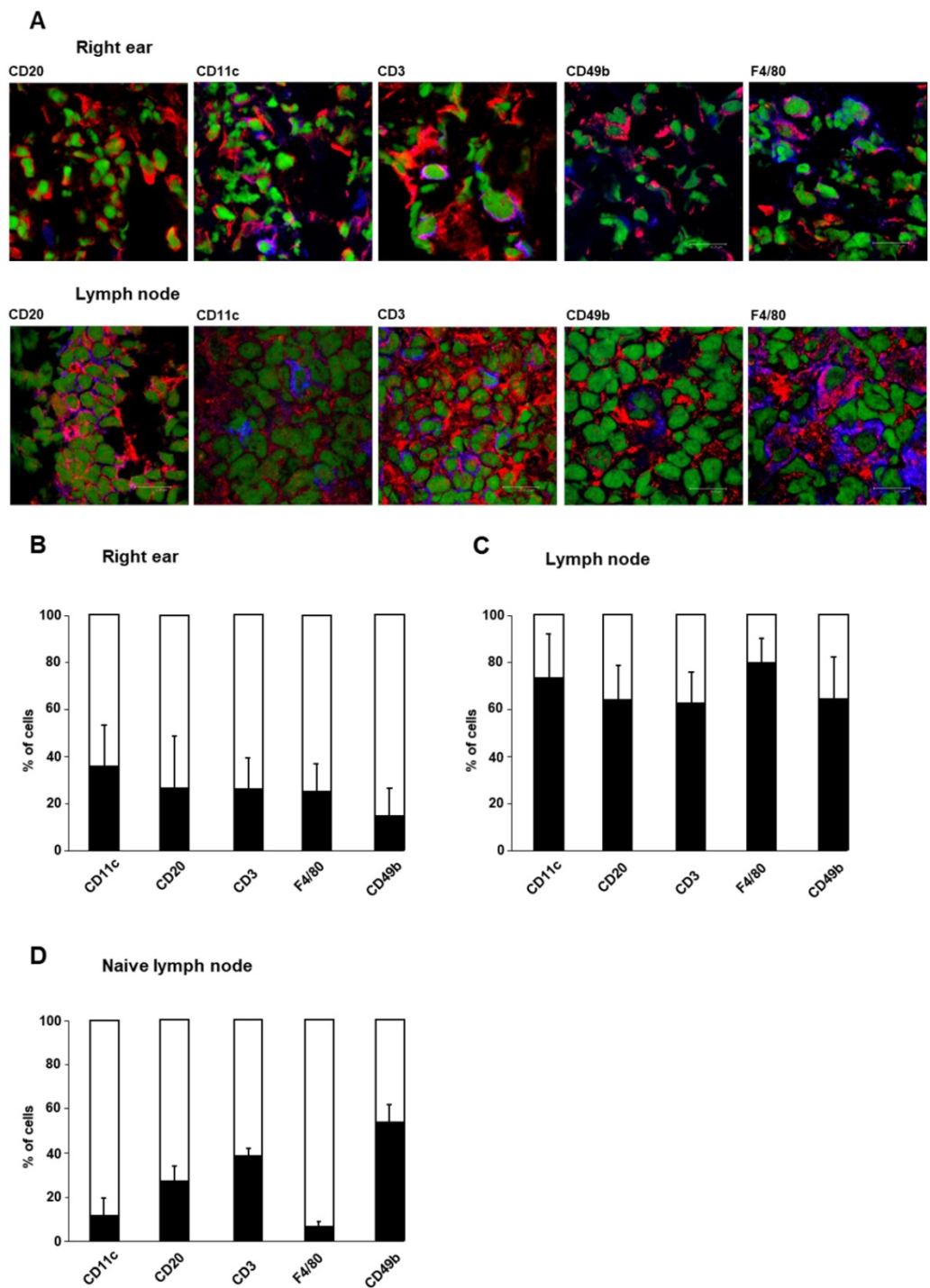


Figure 2: Cellular sources of cathepsin B. Cellular sources of cathepsin B were analyzed by immunofluorescence microscopy using staining with a cathepsin B-specific antibody. The cell types of cathepsin B-expressing cells were determined by antibodies against specific surface antigens. **A:** Immunofluorescence staining of cathepsin B (red) and specific cell surface antigens (blue) in tissue from the right ear and draining lymph nodes of sensitized mice 24 h after TNCB challenge allowed the identification of cathepsin B-expressing immune cells (green represents nuclei). Cells with both antibodies bound appear purple. **B:** Cells onto which both anti-cathepsin B- and anti-cell surface antigen antibodies bound (purple), were counted. The results are shown as the percentage of all cells expressing the specific cell surface antigen (blue+purple). At the site of inflammation (the right ear) in sensitized mice 24 h after TNCB challenge, CD11c-positive dendritic cells exhibited the highest percentage of cells expressing cathepsin B, while CD49b-positive NK cells expressed cathepsin B most rarely among the immune cell populations (n=4; mean±SEM). **C:** In draining lymph nodes of sensitized mice 24 h after TNCB challenge, the percentage of cells expressing cathepsin B was higher than that in inflamed ear tissue. Almost 80% of the F4/80-positive macrophages expressed cathepsin B, while only a few cells in the other populations produced cathepsin B (n=4; mean±SEM). **D:** In cervical lymph nodes of naïve mice, 53% of the CD49b-positive NK cells expressed cathepsin B, while the expression of cathepsin B in F4/80-positive macrophages and CD11c-positive dendritic cells was comparatively low (n=2 mean±SEM).

To exclude potential off-target effects of CA-074, we tested the anti-inflammatory potential of a second cathepsin B inhibitor. We selected the recently developed inhibitor 17, which strongly differs from

CA-074 in its chemical characteristics and exhibited potent inhibitory effects on cathepsin B *in vitro* [22]. Inhibitor 17 reduced ear swelling in acute cutaneous DTHR most effectively at 24 h after the TCNB

challenge (Figure S3A). At this time point, H&E histology of the ears derived from sham- or inhibitor 17-treated mice confirmed reduced edema and leukocyte infiltration as a consequence of inhibitor 17 treatment (Figure S3B).

Active site labeling confirms the therapeutic inhibition of cathepsin B

We chose to use *ex vivo* active site labeling of cysteine-type cathepsins to demonstrate sufficient specific cathepsin B inhibition by CA-074 during acute cutaneous DTHR. Thus, we labeled protease active sites using the activity-based probe DCG-04 [30], which was developed from the broad-spectrum cathepsin inhibitor E-64d. First, we labeled lysates of inflamed ear tissue obtained from mice 24 h after a single TNCB challenge. Competitive labeling with E-64d, which does not produce a signal in this assay, revealed signal suppression by E-64d in several bands, thereby indicating the positions of active cathepsins on the gels (Figure 4C). Treatment of mice with the covalently binding cathepsin B inhibitor CA-074 abolished DCG-04 labeling of a single band, thereby identifying cathepsin B and proving selective inhibition of this protease *in vivo*. Hence, active cathepsin B was present at the site of the inflammatory process, i.e., the ear (Figure 4C). Interestingly, the level of active cathepsin B in draining lymph nodes revealed much stronger cathepsin B activity than that in inflamed ear tissue (Figure 4D). Again, CA-074 treatment effectively reduced active cathepsin B levels in draining lymph nodes during cutaneous DTHR, confirming the

efficacy of selective, irreversible cathepsin B inhibition by CA-074 (Figure 4D). Nevertheless, active site labeling could not assess the inhibitory effect of inhibitor 17, most likely because of the reversible binding mode of inhibitor 17 to cathepsin B (Figure S3C/D). Most importantly, the expression of cathepsin Z in inflamed ears of CA-074 treated mice remained unaffected (Figure S4).

Role of cathepsin Z in *Ctsb*^{-/-} mice

Despite the known proinflammatory role of cathepsin B, *Ctsb*^{-/-} mice revealed an enhanced ear swelling response compared to that of wild-type mice during acute cutaneous DTHR, especially 24 h after challenge (Figure 5A). The absence of cathepsin B may be compensated by another protease. Since cathepsin Z (also known as cathepsin X) is the other carboxypeptidase in the cysteine-type cathepsin family, and because compensatory expression of those proteases has been reported previously [31], we analyzed cathepsin Z in more detail. In sharp contrast to *Ctsb*^{-/-} mice, *Ctsz*^{-/-} mice exhibited a trend towards reduced ear swelling responses 12 h and 24 h after TNCB ear challenge compared with those of wild-type mice (Figure 5A). H&E staining of ear tissue obtained from *Ctsb*^{-/-} mice 24 h after TNCB ear challenge revealed more severe ear swelling, more pronounced edema and a higher density of infiltrating neutrophils than in wild-type mice. However, we could not identify any histopathological differences between *Ctsz*^{-/-} and wild-type mice (Figure 5B).

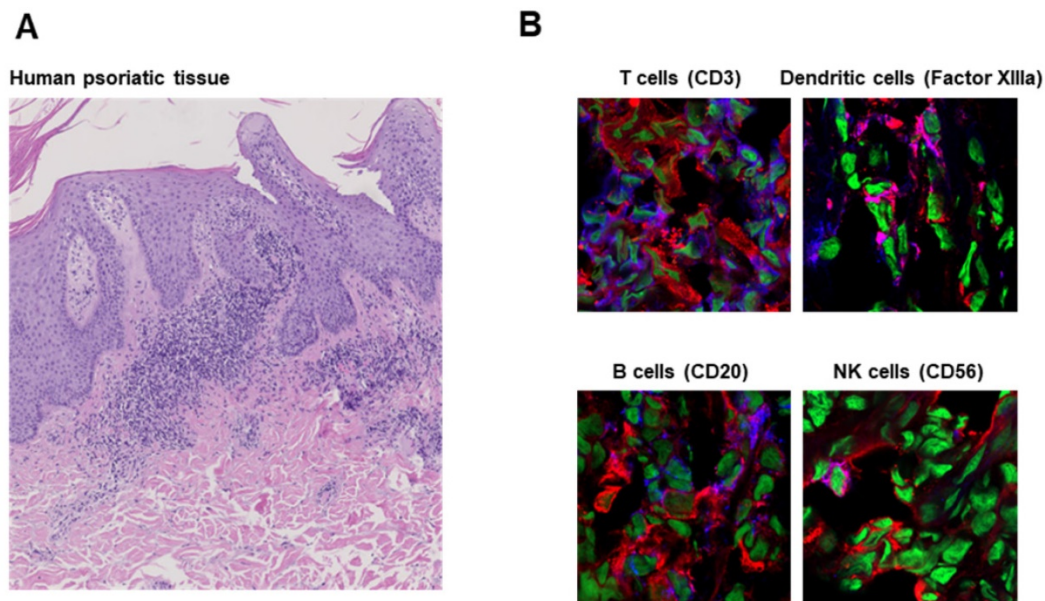


Figure 3: Cathepsin B expression in human inflammatory disease. A: H&E staining of human psoriatic skin tissue obtained from a clinically indicated punch biopsy shows parakeratosis and a dense neutrophil infiltrate. **B:** Immunofluorescence microscopy revealed cathepsin B expression by T cells (CD3), dendritic cells (Factor XIIIa), B cells (CD20) and NK cells (CD56) comparable to that in tissue from mice with experimental acute cutaneous DTHR (Figure 2). Cathepsin B (red); nuclei (green), CD3/Factor XIIIa/CD20/CD56 (blue); cathepsin B and CD3/Factor XIIIa/CD20/CD56 double-positive cells (pink).

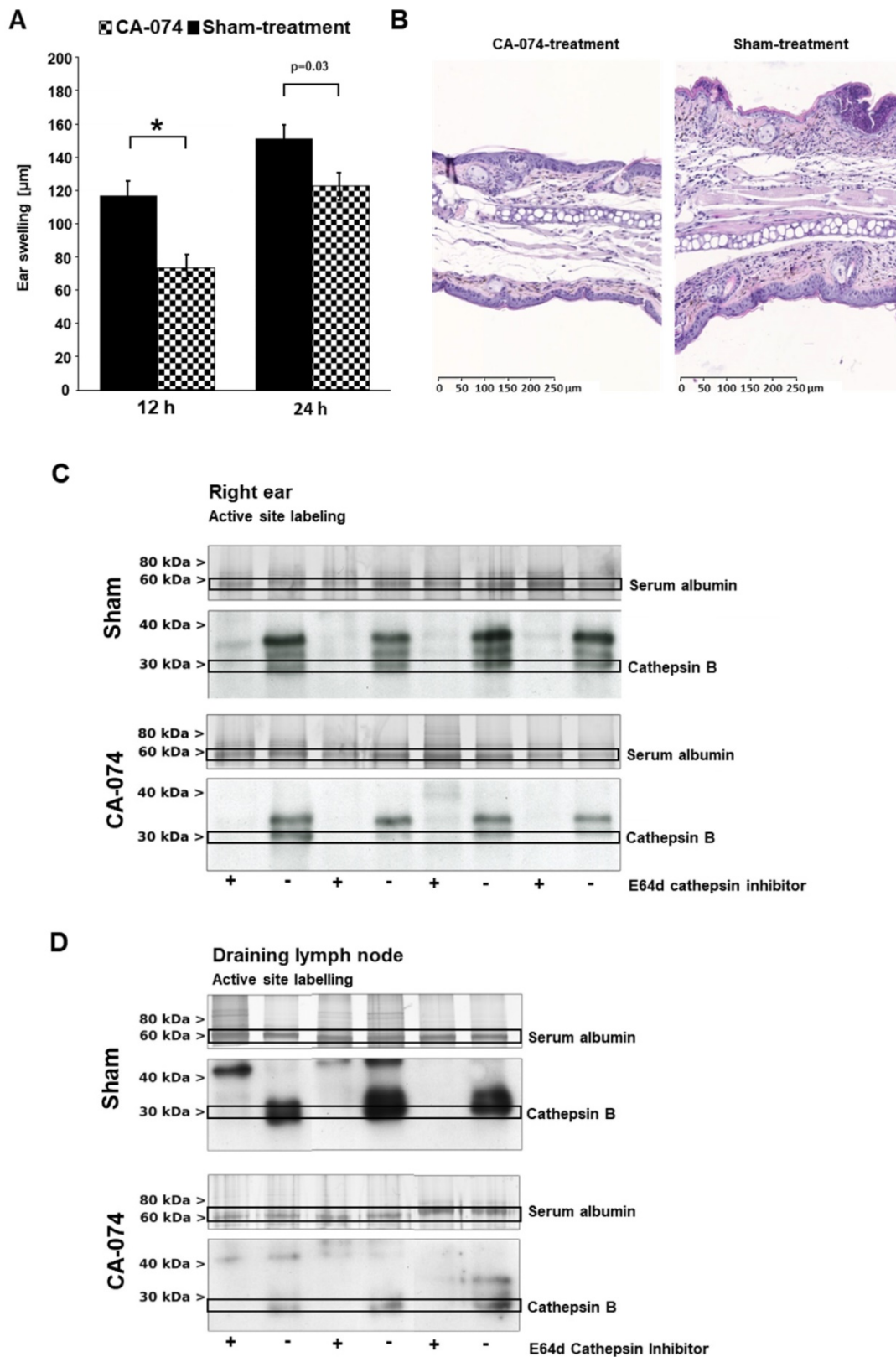


Figure 4: Therapeutic impact of the specific cathepsin B inhibitor CA-074. The specific cathepsin B inhibitor CA-074 or a sham-treatment was applied topically on the right ears daily, starting three days prior the first challenge. **A:** CA-074-treated mice showed a highly significant decrease in ear swelling responses 12 h after the first challenge. Twenty-four hours after the first challenge, the effect on the ear swelling response was lower but still significant (treatment group: n=14; control groups: 12 h, n=28; 24 h, n=25; unpaired, two-tailed Student's t-test; Bonferroni correction for multiple comparisons, significance level $p < 0.0125$; mean \pm SEM). **B:** Ear tissue was harvested 24 h after challenge and stained with H&E according to standard protocols. Tissue from CA-074-treated mice showed noticeably reduced ear thickness and reduced edema, hyperkeratosis, acanthosis and inflammatory cell infiltration (magnification 100x). **C:** To analyze active cathepsin B *in vitro* in tissue harvested from inflamed ears and draining lymph nodes of sensitized mice 24 h after TNCB challenge, we used an activity-based probe, which is an analog of broad-spectrum cysteine-type cathepsin inhibitor the E-64. Active site labeling of probes in inflamed ear tissue revealed active cathepsin B during acute cutaneous DTHR in sham-treated mice. Targeted CA-074 treatment reduced active cathepsin B levels very effectively. **D:** CA-074 strongly suppressed cathepsin B activation in draining lymph nodes.

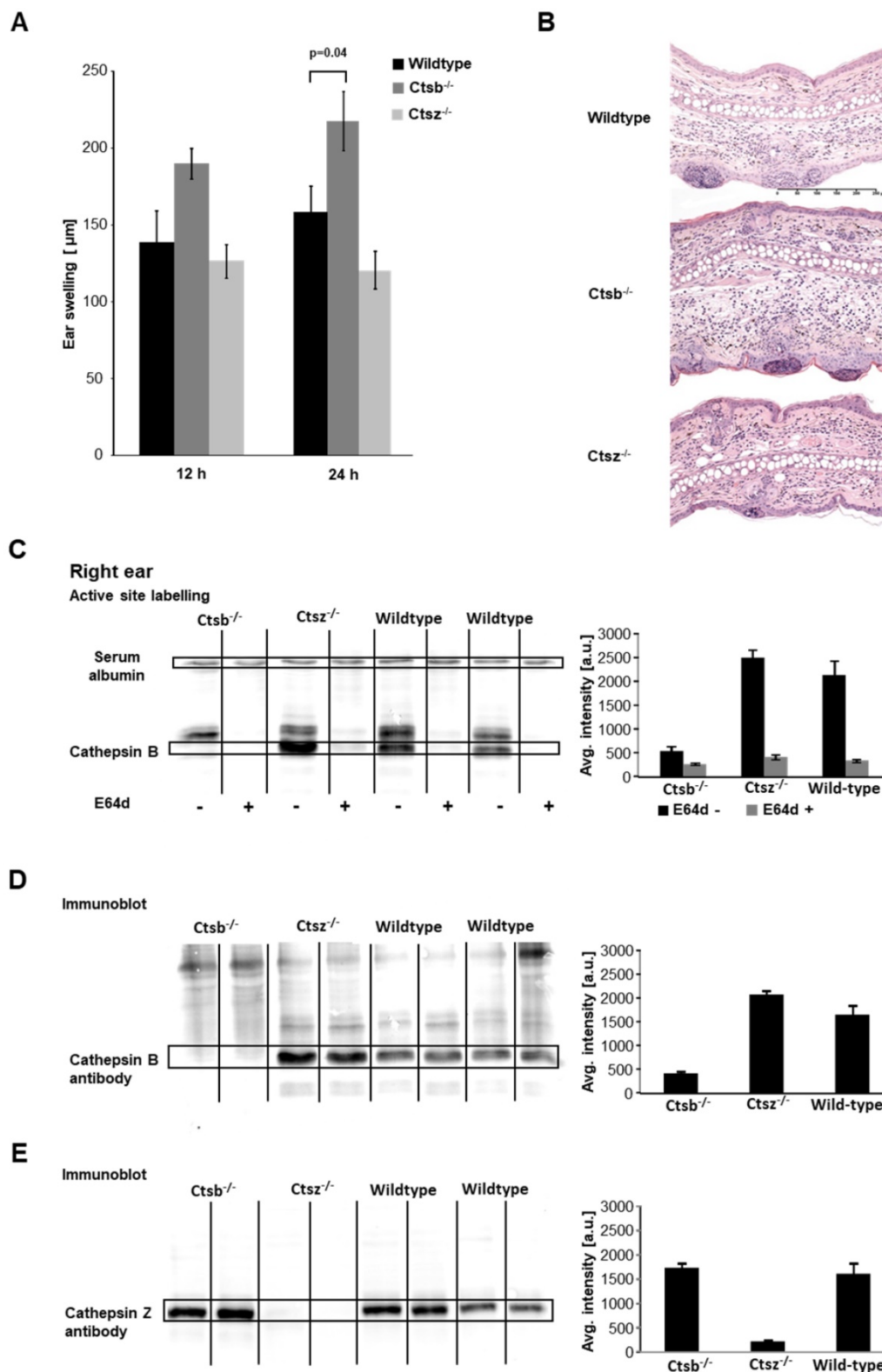


Figure 5: Effect of cathepsin B deficiency. Ctsb^{-/-} mice, Ctsz^{-/-} mice and wild-type mice were sensitized on the abdomen with 5% TNBC and challenged seven days later on the right ear. **A:** We observed significantly enhanced ear swelling in Ctsb^{-/-} mice during acute cutaneous DTHR 24 h after challenge compared to that in wild-type mice, while Ctsz^{-/-} mice showed a trend towards reduced ear swelling compared to that in wild-type mice (wild-type: n=8; Ctsb^{-/-} mice: n=11; Ctsz^{-/-} mice: n=3; two-tailed Student's t-test with Bonferroni correction p < 0.025; mean±SEM). **B:** H&E staining of inflamed ear tissue harvested 24 h after TNBC challenge revealed more severe ear swelling, more pronounced edema and a higher density of infiltrating neutrophils in Ctsb^{-/-} mice than in wild-type mice. However, Ctsz^{-/-} and wild-type mice exhibited no histopathological differences. **C:** Active site labeling revealed a diminished cathepsin B-sized band in the lanes corresponding to samples from Ctsb^{-/-} mice. The cathepsin B bands in the lanes corresponding to samples from Ctsb^{-/-} mice were more prominent than those in the lanes corresponding to samples from wild-type mice, suggesting upregulation of cathepsin B expression (Ctsb^{-/-}: n=4; Ctsz^{-/-}: n=3; wild-type: n=4). **D:** To confirm the identity of the bands detected by active site labeling, we performed immunoblotting on the same gel using a cathepsin B-specific antibody. Immunoblotting indicated a trend towards enhanced cathepsin B expression in Ctsz^{-/-} mice and verified diminished cathepsin B expression in Ctsb^{-/-} mice (Ctsb^{-/-}: n=4; Ctsz^{-/-}: n=3; wild-type: n=4). **E:** Immunoblotting using a cathepsin Z-specific antibody demonstrated a slight trend towards elevated cathepsin Z expression in some Ctsb^{-/-} mice and virtually no cathepsin Z expression in Ctsz^{-/-} mice (Ctsb^{-/-}: n=4; Ctsz^{-/-}: n=3; wild-type: n=4).

Optical imaging using the CatB680 probe during acute TNCB-induced cutaneous DTHR revealed a tendency towards increased signal intensity in the inflamed right ears of *Ctsb*^{-/-} mice compared with that in wild-type mice (Figure S5A), suggesting compensatory effects of other proteases, especially since fluorescence microscopy analysis (Figure S5B) as well as Western blot analysis for cathepsin B expression showed cathepsin B deficiency in the inflamed ears of *Ctsb*^{-/-} mice (Figure 5D).

One day after the first TNCB ear challenge, DCG-04 labeling of ear tissue from *Ctsb*^{-/-} mice revealed markedly reduced cysteine-type cathepsin activity in the region where cathepsin B activity was expected, while cathepsin B was detectable in wild-type and *Ctsz*^{-/-} mice (Figure 5C). Western blot analysis using cathepsin B- and cathepsin Z-specific antibodies clearly identified the cathepsin B- and cathepsin Z-expressing bands that were detected with active site labeling (Figure 5C/D). Interestingly, the cathepsin B immunoblots revealed a trend towards reinforced cathepsin B bands in the lanes corresponding to samples from the inflamed ears of *Ctsz*^{-/-} mice compared to those of wild-type mice, whereas, consistent with our expectations, no cathepsin B-positive band was detectable in samples from *Ctsb*^{-/-} mice (Figure 5D). A similar effect was observed on the cathepsin Z immunoblots: We determined a pronounced cathepsin Z band in the lanes corresponding to samples from the inflamed ears of *Ctsb*^{-/-} mice compared to those of wild-type mice, while *Ctsz*^{-/-} mice did not express cathepsin Z (Figure 5E). These results suggest a compensatory role for cathepsin Z in *Ctsb*^{-/-} mice and may explain the proinflammatory effects in *Ctsb*^{-/-} mice. Analysis of cathepsins in draining lymph nodes revealed a similar level of cathepsin Z expression in *Ctsb*^{-/-} mice and wild-type mice; similarly, no differences in cathepsin B expression were seen between *Ctsz*^{-/-} and wild-type mice (Figure S5C-E).

To test whether cathepsin B or cathepsin Z deficiency differentially impairs the immune system of *Ctsb*^{-/-} and *Ctsz*^{-/-} mice, we first analyzed the cellular composition of the spleen and the inguinal and axillary lymph nodes at the site of abdominal TNCB sensitization by flow cytometry, mainly focusing on CD4⁺ T helper cells and CD8⁺ cytotoxic T cells. Neither *Ctsb*^{-/-} nor *Ctsz*^{-/-} mice (naïve or TNCB-sensitized) exhibited significant alterations in the composition of immune cells or the T cell polarization in the spleen or mesenteric draining lymph nodes (sensitization phase) relative to those factors in wild-type mice with acute cutaneous DTHR (Figure S6).

Discussion

In this study, we examined the importance of the activity of proteases such as cathepsin B in cutaneous DTHR and the resulting implications for future therapeutic strategies.

Proteases play an essential role in different steps of inflammatory process establishment. Cathepsins, a diverse group comprising approximately 15 cysteine, serine or aspartic proteases, are mainly active in the acidic environment of endolysosomes, where they are involved in processing the MHC class II-associated invariant chain and MHC-bound antigens [4]. While cathepsins B and D are not essential for MHC-dependent antigen processing [32], cathepsin S is indispensable for processing antigens and the invariant chain [33]. The ubiquitously expressed cathepsin B is considered a key enzyme in the degradation of immune complexes bound to Fcγ receptors (FcγRs) on antigen-presenting cells (APCs) [34].

In addition to the intracellular roles of cathepsin B, many of its extracellular functions, such as the extracellular matrix degradation and angiogenesis, have been described [8, 9], although the neutral pH outside of the lysosome leads to the inactivation and instability of the cathepsin B molecule [35]. The ability of heparin to prevent pH-dependent cathepsin B degradation has been described [36]. In addition to the proteolytic effect of cathepsin B itself, this enzyme can inactivate inhibitors of MMPs, which are other highly potent mediators of extracellular matrix degradation and angiogenesis [37].

We recently established *in vivo* optical imaging as a tool to noninvasively assess the activity of MMPs in cutaneous DTHR [18]. In this study, we measured high *in vivo* protease activity in ears with chronic cutaneous DTHR using a ProSense probe (Figure 1 A/B). ProSense probes contain an oligo-L-lysine sequence with attached near-infrared fluorochromes and methoxypolyethylene glycol side chains [38]. The oligo-L-lysine sequence is cleaved not only by several cathepsins but also by the proteases trypsin, urokinase and plasmin [37, 39].

Furthermore, we evaluated the CatB680 probe, which is more specific for cathepsins than the ProSense probe [29]. Our measurements revealed a 4-fold enhancement of *in vivo* CatB680 signal intensity in ears (right side) with acute cutaneous DTHR compared with that in healthy control ears (left side). Ears with chronic cutaneous DTHR exhibited a further increase in the CatB680 signal intensity (Figure 1C/D).

CatB680 is cleaved preferentially by cathepsin B; however, Lin et al. reported substantial cleavage by cathepsin S but only a very faint interaction with

cathepsins L, D and K [29]. Cathepsin S is mostly expressed by APCs such as dendritic cells as well as macrophages [4] and is more stable than cathepsin B at neutral pH [40]. Therefore, a considerable contribution of cathepsin S to the cleavage of the CatB680 probe seems plausible.

Various probes for noninvasive *in vivo* imaging of cathepsin B activity are available, for example, nanoparticles with linkers to quenched fluorescent dyes [41], lysosome targeting groups [42] or prodrug-inspired probes [43]. Nevertheless, substrate-like activatable probes are dependent on cleavage sites consisting of peptide sequences that are not exclusively cleaved by one single protease (such as cathepsin B) since active sites are highly conserved throughout the cathepsin family [2, 44]. Caculitan et al. investigated an antibody-drug conjugate with a linker domain designed to be cleaved by cathepsin B, which should lead to the specific release of a cytotoxic drug in the target tissue. Their experiments revealed multiple approaches to produce active catabolites from the antibody-drug conjugate and demonstrated that cathepsin B is dispensable for the cleavage of this linker [45].

Cathepsin inhibitors, antibodies or designed ankyrin repeat proteins (DARPs) [46] labeled with fluorophores or radioactive isotopes can be highly specific but do not reflect the actual proteolytic activity of cysteine-type cathepsins such as cathepsin B. Activity-based probes combine both principles; such probes bind specifically to the protease after activation by proteolytic cleavage [44, 47, 48] but lack signal amplification, as a protease molecule can cleave multiple molecules of a substrate-like activatable probe.

Unfortunately, most of the available probes have not been thoroughly evaluated *in vivo* by specific inhibitor treatment or gene knockout in mice. Our optical imaging experiments revealed a decreasing trend in the CatB680 signal only in draining lymph nodes and not the inflamed ear tissue of CA-074-treated mice (Figure S2B/C; see discussion below). In *Ctsb*^{-/-} mice, we measured an enhanced CatB680 signal intensity compared with wild-type mice (Figure S5A; see discussion below).

Data concerning the exact cellular sources of cathepsin B during inflammatory processes are scarce. However, immunofluorescence microscopy and flow cytometry analysis identified neutrophils, dendritic cells, macrophages and lymphocytes as the main cathepsin B-expressing cell populations (Figure 2).

Lautwein et al. detected cathepsin B expression in peripheral monocytes, as well as in stimulated and unstimulated dendritic cells [49]. Cathepsin B expression in T cells and monocytic cells is elevated

after activation and is involved in the migration of these immune cells [50]. In cytotoxic T cells, cathepsin B is found at the cell surface, suggesting that it protects the cell by cleaving secreted perforin [51]. However, in *Ctsb*^{-/-} mice, the function and survival of cytotoxic T cells were not impaired [52]. Thus, Pipkin et al. assumed that other cathepsins assume the functions of cathepsin B [53].

The percentage of cathepsin B-expressing cells was much higher in draining lymph nodes (Figure 2C) than in inflamed ear tissue (Figure 2B), suggesting an important role for cathepsin B in adaptive immunity, as in antigen processing.

In particular, a high percentage of macrophages and dendritic cells showed cathepsin B expression. While cathepsin B in macrophages and dendritic cells is known for its involvement in antigen processing, no data exist on whether cathepsin B is involved in lymphocyte expansion, possibly explaining the high numbers of cathepsin B-expressing B and T cells in draining lymph nodes (Figure 2C). Regarding B cells, Cathepsin B has been shown to be involved in lymphopoiesis [54]. High-throughput sequencing of macrophages, monocytes and neutrophils from fresh mouse tissues revealed expression of cathepsin B as well as cathepsin Z in multiple subsets of macrophages and neutrophils [55].

Interestingly, neutrophil elastase leads to an upregulation of cathepsin B and MMP-2 expression in macrophages [56]. Regarding neutrophils, most evidence suggests that the secretion of granule-derived cathepsin G mediates the killing of certain bacteria [57] and activates proinflammatory cytokines [58]. An important inducer of cathepsin B release in neutrophils is fluid shear stress [59]. In addition, cathepsin B was found to control the persistence of memory CD8⁺ T cells after viral infection [60]. Fewer cells, especially dendritic cells and macrophages, expressed cathepsin B in the lymph nodes of naïve mice than in the lymph nodes of mice with DTHR, suggesting an elevation of cathepsin B expression through inflammatory processes. Only the percentage of cathepsin B-expressing NK cells remained almost unchanged (Figure 2D). NK cell-derived cathepsin B is suggested to protect cells from self-destruction [51].

To elucidate the therapeutic impact of specifically targeting cathepsin B, we treated mice with the selective cathepsin B inhibitor CA-074. In mice with acute cutaneous DTHR, CA-074 reduced the ear swelling 12 h and 24 h after challenge compared with that in sham-treated mice (Figure 4A). The anti-inflammatory effect of CA-074 was confirmed by histological analyses of ear sections, which revealed reductions in ear thickness, edema,

hyperkeratosis, acanthosis and inflammatory cell infiltration in CA-074-treated mice compared with these parameters in sham-treated mice (Figure 4B).

CA-074 binds to the active site and occludes the loop of cathepsin B [61]. CA-074 inhibits cathepsin B most effectively at acidic pH, which is common in lysosomes [62]. The anionic CA-074 molecule was thought to be unable to penetrate the cell membrane and to inhibit only extracellular cathepsin B, but Szpaderska et al. demonstrated that high concentrations of CA-074 can suppress intracellular cathepsin B *in vitro* [63]. Very possibly, cells can ingest increased concentrations of CA-074 via endocytosis. Several *in vivo* experiments confirmed the effectiveness of cathepsin B inhibition by CA-074. In a murine model of leishmaniasis, CA-074 could trigger the switch from a Th2-dominated inflammatory response to a Th1 immune reaction associated with IFN- γ production [64]. In an *in vivo* tumor xenograft model, CA-074 inhibited tumor growth and the metastatic potential of human melanoma [65].

We further analyzed inflamed ear tissue and draining lymph nodes by active site labeling, a highly sensitive *in vitro* method to tag and visualize the active form of enzymes such as cathepsin B [27].

This method revealed the presence of active cathepsin B in inflamed ear tissue (Figure 4C) and even higher levels in draining lymph nodes (Figure 4D). Topical treatment with the cathepsin B inhibitor CA-074 led to a clear reduction in active cathepsin B levels in inflamed ear tissue and draining lymph nodes compared with these levels in sham-treated mice (Figure 4C/D).

The regulatory dynamics of proteases are largely unknown, but it is plausible that in mice treated with a specific inhibitor such as CA-074, compensatory upregulation of other cathepsins may not occur immediately. This delay could explain why the therapeutic effect of CA-074 is present in acute but not in chronic cutaneous DTHR (Figure S2A).

Surprisingly, we observed enhanced acute TNCB-induced cutaneous DTHR in *Ctsb*^{-/-} mice (Figure 5A), despite the disrupted cathepsin B expression confirmed by immunohistochemistry, active site labeling and Western blotting (Figure 5C/D; Figure S3B-D).

In vivo optical imaging using the CatB680 probe in CA-074-treated mice showed, paradoxically, slightly enhanced cathepsin activity (Figure S2B), whereas *ex vivo* cathepsin activity in the lymph nodes was decreased (Figure S1C/D). These results differed from those of our *ex vivo* active site labeling experiments (Figure 4C/D).

As mentioned above, CatB680 also interacts with cathepsin S, as reported previously [29]. The inhibitor

CA-074 acts specifically on cathepsin B; Katunuma reported that CA-074 does not affect cathepsin S [61]. Therefore, cathepsin S may compensate for cathepsin B to cleave the CatB680 probe. However, whether treatment with CA-074 affects the expression of other cathepsins that are able to activate CatB680 has not yet been investigated.

Furthermore, these differences between cathepsin B activity in lymph nodes and ear tissue in our *ex vivo* and *in vivo* studies may also be due to differing cathepsin B activity and expression in diverse cell compartments.

Through tissue homogenization, protease activity in the extracellular space and all intracellular compartments can be detected *in vitro*. Optical imaging of protease-activatable probes was thought to selectively detect extracellular protease activity; nevertheless, Blum et al. showed that a protease-activatable probe could specifically detect protease activity in intracellular lysosomes *in vitro* [16]. Whether protease-activatable optical imaging probes are internalized into lysosomes or can penetrate the cell membrane remains unknown.

Several cathepsins, such as cathepsins S and L, have endopeptidase functions like those of cathepsin B [66]. Orłowski et al. revealed a redundant function of cathepsins B, L, C, S and X in pro-IL-1 β synthesis and NLRP3-mediated IL-1 β activation [67]. This redundancy suggests that a compensatory function of other cathepsins could be the reason for the undiminished cutaneous DTHR in *Ctsb*^{-/-} mice. Interestingly, optical imaging using CatB680 in *Ctsb*^{-/-} mice showed a higher signal intensity than that in wild-type mice (Figure S5A). Lin et al. showed that CatB680 is mainly activated by cathepsin B but also, to a lesser extent, by cathepsin S [29].

Our results suggest that cathepsin Z may compensate for cathepsin B deficiency in *Ctsb*^{-/-} mice (Figure 5C/D). Both cathepsin Z and cathepsin B are carboxypeptidases in the family of cysteine-type cathepsins and are, therefore, quite similar biochemically [2]. Functionally, cathepsin B is considered an endopeptidase and a carboxydipeptidase [68], whereas cathepsin Z is considered a carboxymonopeptidase [69]. A compensatory role for cathepsin Z in cathepsin B deficiency was previously studied by Vasiljeva et al. [31] and Sevenich et al. [24] in an experimental breast cancer model. To our knowledge, however, this study is the first to investigate the role of cathepsin B and cathepsin Z together in inflammation.

Conclusions

Cysteine-type cathepsins such as cathepsin B are involved in various steps of inflammatory immune

response establishment, especially in draining lymph nodes but also at the site of inflammation. We found that cathepsin B is highly expressed in draining lymph nodes and that the therapeutic effects on active cathepsin B occur mainly in draining lymph nodes. Topical treatment with CA-074, a highly specific cathepsin B inhibitor, revealed a significant anti-inflammatory effect in acute but not chronic cutaneous DTHR. Topically applied cathepsin B inhibitors may reflect a new therapeutic tool for inflammatory skin diseases such as psoriasis.

Abbreviations

ANOVA: analysis of variance; APC: antigen-presenting cells; CHSR: contact hypersensitivity reaction; DARPin: designed ankyrin repeat protein; DC: dendritic cell; DMSO: dimethylsulfoxide; DTHR: delayed-type hypersensitivity reactions; FRET: fluorescence resonance energy transfer; H&E: hematoxylin and eosin; IFN: interferon; MHC: major histocompatibility complex; MMP: matrix metalloproteinase; NLRP: NACHT, LRR and PYD domains-containing protein; PBS: phosphate-buffered saline; ROI: region of interest; SEM: standard error of the mean; SI: signal intensity; Tc: cytotoxic T cell; Th: T helper cell; TLR: Toll-like receptor; TNCB: 2,4,6-trinitrochlorobenzene; TNF: tumor necrosis factor.

Supplementary Material

Supplementary figures.

<http://www.thno.org/v09p3903s1.pdf>

Acknowledgments

The authors thank Maren Harant, Linda Schramm, Ramona Stumm and Funda Cay for providing excellent technical support, as well as Gregory Bowden for providing language editing.

Funding

This work was supported by the Medical Faculty of the Eberhard Karls University Tübingen ("Promotionskolleg" and "PATE-Programm"), the German Research Foundation (SFB TRR156, TP C03 to M.K. & J.S. and TP B07 to K.G.) and the Werner Siemens-Foundation.

Author contributions

J.S., A.M., B.F., R.M., P.K., N.M., D.H., D.B., J.H., I.G.M and M.K. performed the experiments. J.S., A.M., B.F., R.M., P.K., L.Q.-F. and M.K. analyzed the data. J.S. and M.K. wrote the manuscript. A.M., K.F., C.M.G., M.S., K.G., L.Q.-F., M.G., S.L., T.R., M.R., H.K. and B.J.P. contributed technical expertise and

critically edited the manuscript. All authors read and approved the manuscript.

Competing Interests

The authors have declared that no competing interest exists.

References

- Reiser J, Adair B, Reinheckel T. Specialized roles for cysteine cathepsins in health and disease. *J Clin Invest.* 2010; 120: 3421-31.
- Turk V, Stoka V, Vasiljeva O, Renko M, Sun T, Turk B, et al. Cysteine cathepsins: from structure, function and regulation to new frontiers. *Biochim Biophys Acta.* 2012; 1824: 68-88.
- Turk V, Stoka V, Vasiljeva O, Renko M, Sun T, Turk B, et al. Cysteine cathepsins: from structure, function and regulation to new frontiers. *Biochim Biophys Acta.* 2012; 1824: 68-88.
- Honey K, Rudensky AY. Lysosomal cysteine proteases regulate antigen presentation. *Nat Rev Immunol.* 2003; 3: 472-82.
- Conus S, Simon HU. Cathepsins and their involvement in immune responses. *Swiss Med Wkly.* 2010; 140: w13042.
- Chwieralski CE, Welte T, Buhling F. Cathepsin-regulated apoptosis. *Apoptosis.* 2006; 11: 143-9.
- Ha SD, Martins A, Khazaie K, Han J, Chan BM, Kim SO. Cathepsin B is involved in the trafficking of TNF-alpha-containing vesicles to the plasma membrane in macrophages. *J Immunol.* 2008; 181: 690-7.
- Im E, Venkatakrishnan A, Kazlauskas A. Cathepsin B regulates the intrinsic angiogenic threshold of endothelial cells. *Mol Biol Cell.* 2005; 16: 3488-500.
- Obermajer N, Jevnikar Z, Doljak B, Kos J. Role of cysteine cathepsins in matrix degradation and cell signalling. *Connect Tissue Res.* 2008; 49: 193-6.
- Hashimoto Y, Kakegawa H, Narita Y, Hachiya Y, Hayakawa T, Kos J, et al. Significance of cathepsin B accumulation in synovial fluid of rheumatoid arthritis. *Biochem Biophys Res Commun.* 2001; 283: 334-9.
- Bever CT, Jr., Garver DW. Increased cathepsin B activity in multiple sclerosis brain. *J Neurol Sci.* 1995; 131: 71-3.
- Van Acker GJ, Saluja AK, Bhagat L, Singh VP, Song AM, Steer ML. Cathepsin B inhibition prevents trypsinogen activation and reduces pancreatitis severity. *Am J Physiol Gastrointest Liver Physiol.* 2002; 283: G794-800.
- Mohamed MM, Sloane BF. Cysteine cathepsins: multifunctional enzymes in cancer. *Nat Rev Cancer.* 2006; 6: 764-75.
- Hook V, Schechter I, Demuth HU, Hook G. Alternative pathways for production of beta-amyloid peptides of Alzheimer's disease. *Biol Chem.* 2008; 389: 993-1006.
- Ntziachristos V, Tung CH, Bremer C, Weissleder R. Fluorescence molecular tomography resolves protease activity in vivo. *Nat Med.* 2002; 8: 757-60.
- Blum G, von Degenfeld G, Merchant MJ, Blau HM, Bogyo M. Noninvasive optical imaging of cysteine protease activity using fluorescently quenched activity-based probes. *Nat Chem Biol.* 2007; 3: 668-77.
- Kneilling M, Mailhammer R, Hultner L, Schonberger T, Fuchs K, Schaller M, et al. Direct crosstalk between mast cell-TNF and TNFR1-expressing endothelia mediates local tissue inflammation. *Blood.* 2009; 114: 1696-706.
- Schwenck J, Griessinger CM, Fuchs K, Bukala D, Bauer N, Eichner M, et al. In vivo optical imaging of matrix metalloproteinase activity detects acute and chronic contact hypersensitivity reactions and enables monitoring of the antiinflammatory effects of N-acetylcysteine. *Mol Imaging.* 2014: 1-12.
- Pichler BJ, Kneilling M, Haubner R, Braumuller H, Schwaiger M, Rocken M, et al. Imaging of delayed-type hypersensitivity reaction by PET and 18F-galacto-RGD. *J Nucl Med.* 2005; 46: 184-9.
- Murata M, Miyashita S, Yokoo C, Tamai M, Hanada K, Hatayama K, et al. Novel epoxysuccinyl peptides. Selective inhibitors of cathepsin B, in vitro. *FEBS Lett.* 1991; 280: 307-10.
- Montaser M, Lalmanach G, Mach L. CA-074, but not its methyl ester CA-074Me, is a selective inhibitor of cathepsin B within living cells. *Biol Chem.* 2002; 383: 1305-8.
- Schmitz J, Li T, Bartz U, Gutschow M. Cathepsin B Inhibitors: Combining Dipeptide Nitriles with an Occluding Loop Recognition Element by Click Chemistry. *ACS Med Chem Lett.* 2016; 7: 211-6.
- Halangk W, Lerch MM, Brandt-Nedelev B, Roth W, Ruthenbuenger M, Reinheckel T, et al. Role of cathepsin B in intracellular trypsinogen activation and the onset of acute pancreatitis. *J Clin Invest.* 2000; 106: 773-81.
- Sevenich L, Schurigt U, Sachse K, Gajda M, Werner F, Muller S, et al. Synergistic antitumor effects of combined cathepsin B and cathepsin Z deficiencies on breast cancer progression and metastasis in mice. *Proc Natl Acad Sci U S A.* 2010; 107: 2497-502.
- Schmitz J, Li TW, Bartz U, Gutschow M. Cathepsin B Inhibitors: Combining Dipeptide Nitriles with an Occluding Loop Recognition Element by Click Chemistry. *ACS Med Chem Lett.* 2016; 7: 211-6.
- Biedermann T, Kneilling M, Mailhammer R, Maier K, Sander CA, Kollias G, et al. Mast cells control neutrophil recruitment during T cell-mediated delayed-type hypersensitivity reactions through tumor necrosis factor and macrophage inflammatory protein 2. *J Exp Med.* 2000; 192: 1441-52.

27. Lutzner N, Kalbacher H. Quantifying cathepsin S activity in antigen presenting cells using a novel specific substrate. *J Biol Chem.* 2008; 283: 36185-94.
28. Nahrendorf M, Waterman P, Thurber G, Groves K, Rajopadhye M, Panizzi P, et al. Hybrid in vivo FMT-CT imaging of protease activity in atherosclerosis with customized nanosensors. *Arterioscler Thromb Vasc Biol.* 2009; 29: 1444-51.
29. Lin SA, Patel M, Suresch D, Connolly B, Bao B, Groves K, et al. Quantitative Longitudinal Imaging of Vascular Inflammation and Treatment by Ezetimibe in apoE Mice by FMT Using New Optical Imaging Biomarkers of Cathepsin Activity and alpha(v)beta(3) Integrin. *Int J Mol Imaging.* 2012; 2012: 189254.
30. Greenbaum D, Medzhradszky KF, Burlingame A, Bogyo M. Epoxide electrophiles as activity-dependent cysteine protease profiling and discovery tools. *Chem Biol.* 2000; 7: 569-81.
31. Vasiljeva O, Papazoglou A, Kruger A, Brodoefel H, Korovin M, Deussing J, et al. Tumor cell-derived and macrophage-derived cathepsin B promotes progression and lung metastasis of mammary cancer. *Cancer Res.* 2006; 66: 5242-50.
32. Deussing J, Roth W, Saftig P, Peters C, Ploegh HL, Villadangos JA. Cathepsins B and D are dispensable for major histocompatibility complex class II-mediated antigen presentation. *Proc Natl Acad Sci U S A.* 1998; 95: 4516-21.
33. Riese RJ, Wolf PR, Bromme D, Natkin LR, Villadangos JA, Ploegh HL, et al. Essential role for cathepsin S in MHC class II-associated invariant chain processing and peptide loading. *Immunity.* 1996; 4: 357-66.
34. Driessen C, Lennon-Dumenil AM, Ploegh HL. Individual cathepsins degrade immune complexes internalized by antigen-presenting cells via Fc gamma receptors. *Eur J Immunol.* 2001; 31: 1592-601.
35. Puzer L, Cotrin SS, Cezari MH, Hirata IY, Juliano MA, Stefe I, et al. Recombinant human cathepsin X is a carboxymonopeptidase only: a comparison with cathepsins B and L. *Biological chemistry.* 2005; 386: 1191-5.
36. Costa MGS, Batista PR, Shida CS, Robert CH, Bisch PM, Pascutti PG. How does heparin prevent the pH inactivation of cathepsin B? Allosteric mechanism elucidated by docking and molecular dynamics. *BMC Genomics.* 2010; 11.
37. Kostoulas G, Lang A, Nagase H, Baici A. Stimulation of angiogenesis through cathepsin B inactivation of the tissue inhibitors of matrix metalloproteinases. *FEBS Lett.* 1999; 455: 286-90.
38. Weissleder R, Tung CH, Mahmood U, Bogdanov A, Jr. In vivo imaging of tumors with protease-activated near-infrared fluorescent probes. *Nat Biotechnol.* 1999; 17: 375-8.
39. Costa MG, Batista PR, Shida CS, Robert CH, Bisch PM, Pascutti PG. How does heparin prevent the pH inactivation of cathepsin B? Allosteric mechanism elucidated by docking and molecular dynamics. *BMC Genomics.* 2010; 11 Suppl 5: S5.
40. Bromme D, Bonneau PR, Lachance P, Wiederanders B, Kirschke H, Peters C, et al. Functional expression of human cathepsin S in *Saccharomyces cerevisiae*. Purification and characterization of the recombinant enzyme. *J Biol Chem.* 1993; 268: 4832-8.
41. Ryu JH, Kim SA, Koo H, Yhee JY, Lee A, Na JH, et al. Cathepsin B-sensitive nanoprobe for in vivo tumor diagnosis. *J Mater Chem.* 2011; 21: 17631-4.
42. Wang YQ, Li JB, Feng LD, Yu JF, Zhang Y, Ye DJ, et al. Lysosome-Targeting Fluorogenic Probe for Cathepsin B Imaging in Living Cells. *Anal Chem.* 2016; 88: 12403-10.
43. Chowdhury MA, Moya IA, Bhilocha S, McMillan CC, Vigliarolo BG, Zehbe I, et al. Prodrug-inspired probes selective to cathepsin B over other cysteine cathepsins. *J Med Chem.* 2014; 57: 6092-104.
44. Watzke A, Kosec G, Kindermann M, Jeske V, Nestler HP, Turk V, et al. Selective activity-based probes for cysteine cathepsins. *Angew Chem Int Ed Engl.* 2008; 47: 406-9.
45. Caclutan NG, Dela Cruz Chuh J, Ma Y, Zhang D, Kozak KR, Liu Y, et al. Cathepsin B Is Dispensable for Cellular Processing of Cathepsin B-Cleavable Antibody-Drug Conjugates. *Cancer Res.* 2017; 77: 7027-37.
46. Kramer L, Renko M, Završnik J, Turk D, Seeger MA, Vasiljeva O, et al. Non-invasive in vivo imaging of tumour-associated cathepsin B by a highly selective inhibitory DARPin. *Theranostics.* 2017; 7: 2806-21.
47. Edem PE, Czorny S, Valliant JF. Synthesis and Evaluation of Radioiodinated Acyloxymethyl Ketones as Activity-Based Probes for Cathepsin B. *Journal of Medicinal Chemistry.* 2014; 57: 9564-77.
48. Ren G, Blum G, Verdoes M, Liu HG, Syed S, Edgington LE, et al. Non-Invasive Imaging of Cysteine Cathepsin Activity in Solid Tumors Using a Cu-64-Labeled Activity-Based Probe. *Plos One.* 2011; 6.
49. Lautwein A, Burster T, Lennon-Dumenil AM, Overkleef HS, Weber E, Kalbacher H, et al. Inflammatory stimuli recruit cathepsin activity to late endosomal compartments in human dendritic cells. *Eur J Immunol.* 2002; 32: 3348-57.
50. Staun-Ram E, Miller A. Cathepsins (S and B) and their inhibitor Cystatin C in immune cells: modulation by interferon-beta and role played in cell migration. *J Neuroimmunol.* 2011; 232: 200-6.
51. Balaji KN, Schaschke N, Machleidt W, Catalfamo M, Henkart PA. Surface cathepsin B protects cytotoxic lymphocytes from self-destruction after degranulation. *J Exp Med.* 2002; 196: 493-503.
52. Baran K, Ciccone A, Peters C, Yagita H, Bird PI, Villadangos JA, et al. Cytotoxic T lymphocytes from cathepsin B-deficient mice survive normally in vitro and in vivo after encountering and killing target cells. *J Biol Chem.* 2006; 281: 30485-91.
53. Pipkin ME, Lieberman J. Delivering the kiss of death: progress on understanding how perforin works. *Curr Opin Immunol.* 2007; 19: 301-8.
54. Lalanne AI, Moraga I, Hao Y, Pereira JP, Alves NL, Huntington ND, et al. CpG inhibits pro-B cell expansion through a cathepsin B-dependent mechanism. *J Immunol.* 2010; 184: 5678-85.
55. Lavin Y, Winter D, Blecher-Gonen R, David E, Keren-Shaul H, Merad M, et al. Tissue-resident macrophage enhancer landscapes are shaped by the local microenvironment. *Cell.* 2014; 159: 1312-26.
56. Geraghty P, Rogan MP, Greene CM, Boxio RMM, Poiriert T, O'Mahony M, et al. Neutrophil elastase up-regulates cathepsin B and matrix metalloproteinase-2 expression. *Journal of Immunology.* 2007; 178: 5871-8.
57. van der Windt D, Bootsma HJ, Burghout P, van der Gaast-de Jongh CE, Hermans PW, van der Flier M. Nonencapsulated *Streptococcus pneumoniae* resists extracellular human neutrophil elastase- and cathepsin G-mediated killing. *FEMS Immunol Med Microbiol.* 2012; 66: 445-8.
58. Henry CM, Sullivan GP, Clancy DM, Afonina IS, Kulms D, Martin SJ. Neutrophil-Derived Proteases Escalate Inflammation through Activation of IL-36 Family Cytokines. *Cell Rep.* 2016; 14: 708-22.
59. Akenhead ML, Fukuda S, Schmid-Schonbein GW, Shin HY. Fluid shear-induced cathepsin B release in the control of Mac1-dependent neutrophil adhesion. *J Leukoc Biol.* 2017; 102: 117-26.
60. Byrne SM, Aucher A, Alyahya S, Elder M, Olson ST, Davis DM, et al. Cathepsin B controls the persistence of memory CD8+ T lymphocytes. *J Immunol.* 2012; 189: 1133-43.
61. Katunuma N. Structure-based development of specific inhibitors for individual cathepsins and their medical applications. *Proc Jpn Acad Ser B Phys Biol Sci.* 2011; 87: 29-39.
62. Linebaugh BE, Sameni M, Day NA, Sloane BF, Keppler D. Exocytosis of active cathepsin B enzyme activity at pH 7.0, inhibition and molecular mass. *Eur J Biochem.* 1999; 264: 100-9.
63. Szpadwerska AM, Frankfater A. An intracellular form of cathepsin B contributes to invasiveness in cancer. *Cancer Res.* 2001; 61: 3493-500.
64. Maekawa Y, Himeno K, Ishikawa H, Hisaeda H, Sakai T, Dainichi T, et al. Switch of CD4+ T cell differentiation from Th2 to Th1 by treatment with cathepsin B inhibitor in experimental leishmaniasis. *J Immunol.* 1998; 161: 2120-7.
65. Matarrese P, Ascione B, Ciarlo L, Vona R, Leonetti C, Scarsella M, et al. Cathepsin B inhibition interferes with metastatic potential of human melanoma: an in vitro and in vivo study. *Mol Cancer.* 2010; 9: 207.
66. Olson OC, Joyce JA. Cysteine cathepsin proteases: regulators of cancer progression and therapeutic response. *Nat Rev Cancer.* 2015; 15: 712-29.
67. Orłowski GM, Colbert JD, Sharma S, Bogyo M, Robertson SA, Rock KL. Multiple Cathepsins Promote Pro-IL-1beta Synthesis and NLRP3-Mediated IL-1beta Activation. *J Immunol.* 2015; 195: 1685-97.
68. Musil D, Zucic D, Turk D, Engh RA, Mayr I, Huber R, et al. The refined 2.15 Å X-ray crystal structure of human liver cathepsin B: the structural basis for its specificity. *EMBO J.* 1991; 10: 2321-30.
69. Guncar G, Klemencic I, Turk B, Turk V, Karaoglanovic-Carmona A, Juliano L, et al. Crystal structure of cathepsin X: a flip-flop of the ring of His23 allows carboxy-monopeptidase and carboxy-dipeptidase activity of the protease. *Structure.* 2000; 8: 305-13.